



# Evaluation of hydroxamate-based resins towards a more clinically viable $^{44}\text{Ti}/^{44}\text{Sc}$ radionuclide generator

Leah Gajecki<sup>a,\*</sup>, Celine M. Marino<sup>a,b</sup>, Cathy S. Cutler<sup>a</sup>, Vanessa A. Sanders<sup>a</sup>

<sup>a</sup> Collider Accelerator Department, Brookhaven National Laboratory, Upton, NY, 11973, USA

<sup>b</sup> Chemistry Department, Stony Brook University, Stony Brook, NY, 11794, USA

## ABSTRACT

Several hydroxamate-based resins were synthesized and tested for use in  $^{44}\text{Ti}/^{44}\text{Sc}$  generator systems in small scale experiments (740 kBq  $^{44}\text{Ti}$ ). The most promising resin was tested further in larger scale generator studies (37 MBq). This resin displayed impressive retention of  $^{44}\text{Ti}$  over several elutions, and high quantities of  $^{44}\text{Sc}$  were obtained in small volumes of dilute HCl eluents. Initial radiolabeling experiments were conducted and demonstrated the possibility of direct radiolabeling of the generator produced  $^{44}\text{Sc}$  with DOTA.

## 1. Introduction

Scandium-44 ( $^{44}\text{Sc}$ ) is of high interest as a potential positron emission tomography (PET) imaging radionuclide due to its promising nuclear characteristics such as high positron branching ratio (94.27%) and 3.97 h half-life, making it a suitable candidate for radiolabeling of small to medium biomolecules since it matches their biological half-lives (Muller et al., 2013; Honarvar et al., 2017; Hernansez et al., 2014; Eigner et al., 2013). Additionally,  $^{44}\text{Sc}$  has shown superior image resolution in radiopharmaceutical imaging compared to the analogous  $^{68}\text{Ga}$  systems due to the lower average positron energy (632 keV vs. 830 keV for  $^{44}\text{Sc}$  and  $^{68}\text{Ga}$ , respectively) (Koumariou et al., 2012; Domnanich et al., 2017). Along with these desirable PET imaging radionuclide characteristics,  $^{44}\text{Sc}$  can also be easily obtained by the decay of its long-lived parent isotope titanium-44  $^{44}\text{Ti}$  ( $t_{1/2} = 60.0$  years), whereby a  $^{44}\text{Ti}/^{44}\text{Sc}$  generator system would allow for daily elution of the maximum  $^{44}\text{Sc}$  activity without the need for on-site cyclotrons. Development of an acceptable  $^{44}\text{Ti}/^{44}\text{Sc}$  radionuclide generator needs to address several criteria such as efficient parent-daughter separation, low  $^{44}\text{Ti}$  breakthrough, long term consistent and reliable results (such as consistent  $^{44}\text{Sc}$  elution activity and volumes), and Sc eluates that will be suitable for subsequent radiolabeling (low volume, low pH, high purity). Several current generators employ the use of AG 1-X8 anion exchange resin eluting the scandium with dilute oxalic acid/hydrochloric acid mixtures (Filosofov et al., 2010; Kerdjoudj et al., 2016; Pruszyński et al., 2010; Roesch, 2012). However, there are numerous drawbacks to this method, including: 1) extremely large elution volumes, 2) short generator lifetimes before  $^{44}\text{Ti}$  breakthrough, and 3) the presence of

competing oxalates in solution which hinders subsequent radiolabeling.

More recently the use of commercially available ZR resin has been suggested for use as a possible  $^{44}\text{Ti}/^{44}\text{Sc}$  radionuclide generator system (Holland et al., 2009; Radchenko et al., 2016). This hydroxamate based ZR resin developed by Triskem has been commonly used to separate Zr from Y targets, but unsurprisingly due to the chemical similarities between the Zr(IV)/Y(III) and Ti(IV)/Sc(III) pair, it also shows high selectivity for Ti and little selectivity for Sc over a range of HCl molarities (Dirks et al., 2015; Radchenko et al., 2016). While the high retention of  $^{44}\text{Ti}$  on the ZR resin indeed seems promising, there is little to no information in the literature on the  $^{44}\text{Sc}$  elution activity or generator lifetime. One study conducted by Radchenko et al. suggests  $^{44}\text{Ti}$  breakthrough after 40 bed volume elutions of a conventional direct elution generator, with increased generator lifetime possible by employing a reverse elution mode, previously used in the AG 1-X8  $^{44}\text{Ti}/^{44}\text{Sc}$  generator system (Filosofov et al., 2010; Radchenko et al., 2016). From our own preliminary research using ZR resin based generators, the elution volumes needed compared to the AG 1-X8 generators is drastically decreased, but the time until  $^{44}\text{Ti}$  breakthrough as well as the amount and purity of the  $^{44}\text{Sc}$  elution has been extremely inconsistent and unreliable. As ZR resin is an extraction chromatographic resin it is plausible that there is leaching and deterioration of the extractant over time which could be leading to these discrepancies and would hinder subsequent radiolabeling. While the ZR resin is still a feasible option for a viable  $^{44}\text{Ti}/^{44}\text{Sc}$  generator system, there is much room for improvement to produce a potentially clinically relevant  $^{44}\text{Ti}/^{44}\text{Sc}$  generator system.

The main advantage of the ZR resin is the use of a hydroxamate

\* Corresponding author. P.O. Box 5000, Building #801, Upton, NY, 11973, USA.

E-mail address: [lgajecki@bnl.gov](mailto:lgajecki@bnl.gov) (L. Gajecki).

functional group to create a chelating resin rather than an anion exchange type resin. Chelating resins have the potential to bind much more strongly and selectively to the radioisotope of interest allowing for longer lived generators with lower observed breakthrough. Hydroxamates specifically are well known to bind strongly to Fe(III) in nature in the form of siderophores, bacteria produced chelates, found commonly in seawater (Mawji et al., 2008; Orłowska et al., 2016; Szaniszlo et al., 1981). The similarity in binding behavior of Fe(III) and Ti(IV) has led to several examples of siderophore-like hydroxamate Ti complexes and metal-organic frameworks (MOFs) (Saxena et al., 2018; Brennan et al., 2016; Padial et al., 2019; Passadis et al., 2021; Jones et al., 2017). These examples demonstrate the affinity of hydroxamates to strongly bind Ti (IV) making them very attractive chelates to incorporate into potential  $^{44}\text{Ti}/^{44}\text{Sc}$  generator resins. ZR resin is currently the only commercially available hydroxamate based resin, but there are examples of synthesized hydroxamate and hydroxamic acid based resins in the literature that have been tested to bind a variety of metals, some including Ti(IV) (Phillips and Fritz, 1980, 1982; Petrie et al., 1965; Liu et al., 1992; Khodadadi et al., 1995; Meijs et al., 1994; Herscheid et al., 1983; Agrawal et al., 1999; Cornaz and Deuel, 1954; Cornaz et al., 1957; Holland et al., 2009). None of these resins have been explored as potential resins for  $^{44}\text{Ti}/^{44}\text{Sc}$  generator systems, but one Accell hydroxamate resin was used in the successful separation of Zr(IV) and Y(III), similar to what the ZR resin is used for (Holland et al., 2009). Other functionalized hydroxamate based resins prepared by Phillips and Fritz showed extremely high Ti retention and demonstrated the effect that the substituent on the nitrogen of the hydroxamate has on metal retention (Phillips, 1980; Phillips and Fritz, 1982). It was suggested that a methyl substituted hydroxamate may bind metals (Ti, Fe, Cu, Al, U, and Th) more strongly than unsubstituted and phenyl derivatives. This led to an investigation of a variety of functionalized hydroxamate resins for use in potential  $^{44}\text{Ti}/^{44}\text{Sc}$  generator systems.

## 2. Experimental

### 2.1. Chemicals and reagents

All chemicals were used without further purification. Hydroxylamine hydrochloride, N-methylhydroxylamine hydrochloride, N-phenylhydroxylamine, 2,3,5,6-tetrafluorophenol (TFP), 1-ethyl-3-(3-dimethylaminopropyl)carbodiimide hydrochloride (EDC), potassium hydroxide (KOH),  $\text{SOCl}_2$ , anhydrous diethylether, acetonitrile (ACN), and HPLC grade methanol (MeOH) were purchased from Sigma Aldrich (St. Louis, MO, USA). Optima grade hydrochloric acid (HCl) was purchased from Fisher Scientific (Pittsburgh, PA, USA) and diluted to suitable concentrations (8 M, 6 M, 4 M, 2 M, 0.5 M, 0.1 M) with 18 M $\Omega$  water (25 °C, Milli-Q, Millipore, Burlington, MA, USA). Optima grade nitric acid ( $\text{HNO}_3$ ) was purchased from Fisher Scientific (Pittsburgh, PA, USA) and diluted to 2% with 18 M $\Omega$  water (25 °C, Milli-Q, Millipore, Burlington, MA, USA). Metal solutions of scandium and titanium were prepared from ICP Standards purchased from SPEX Cetiprep (Metuchen, NJ, USA). ZR resin was purchased from Triskem Intl. (Brunz, France), Amberlite IRC50 resin and Amberlite CG50 resin were purchased from Sigma Aldrich and Accell Plus CM resin was purchased from Waters (Milford, MA, USA). Deionized Milli-Q water (18 M $\Omega$ , Millipore) which had been purified by passing through a 10 cm column of Chelex 100 resin (Bio-Rad Laboratories, Hercules, CA, USA) was used in all reactions and solution preparations.

### 2.2. Synthesis of resins

Full synthetic procedures and characterization data of all resins can be found in the Supplementary Materials. All resins were synthesized using literature procedures or modified literature procedures where no literature precedent was found *vide infra*. All resins were characterized by ATIR spectroscopy (Supplementary Materials) and all hydroxamate

resins were qualitatively characterized by visual formation of a dark red complex upon addition of Fe(III) in dilute acid to the resin (Davidson, 1940). All synthesized hydroxamate resins used in further generator studies were given the abbreviations as follows: Accell unsubstituted hydroxamate resin (AU), Accell methyl substituted hydroxamate resin (AM), Accell phenyl substituted hydroxamate resin (AP), IRC50 unsubstituted hydroxamate resin (IU), IRC50 methyl substituted hydroxamate resin (IM), IRC50 phenyl substituted hydroxamate resin (IP), CG50 unsubstituted hydroxamate resin (CU), CG50 methyl substituted hydroxamate resin (CM), CG50 phenyl substituted hydroxamate resin (CP).

### 2.3. Production and purification of $^{44}\text{Ti}$

Production of  $^{44}\text{Ti}$  used in the radionuclide generators was conducted by irradiation of a scandium sputtering target (American Elements) at the Brookhaven Linac Isotope Producer (BLIP). Full production and purification procedures can be found in the Supplementary Materials.

### 2.4. Radiolabeling

The  $^{44}\text{Sc}$  generator eluent (in 0.5 M HCl) was brought to a pH of 4 with dilute NaOH solution, and then used directly (e.g., without post-elution processing) in subsequent labeling reactions. Radiolabeling of generator eluted  $^{44}\text{Sc}$  with DOTA was performed by mixing the ligand stock solution (0.04 mg/mL, 0.25 M  $\text{NH}_4\text{OAc}$  pH 4 buffer) with the neutralized  $^{44}\text{Sc}$  eluent in a 1.5 mL Eppendorf tube and heating the solution at 90 °C for 1 h in a thermomixer. The activity of  $^{44}\text{Sc}$  used in radiolabeling was 925 kBq (25  $\mu\text{Ci}$ ) with 1.59 nmol of DOTA.

The radiolabeling yield was determined using thin-layer chromatography (iTLC-SG strips, Agilent). The plates were developed in 0.04 M  $\text{NH}_4\text{OAc}/\text{MeOH}$  (50/50) pH 5 buffer and were counted for 1 min on a BIOSCAN AR 2000. The  $R_f$  values for the free  $^{44}\text{Sc}$  and labeled  $^{44}\text{Sc}$  were 0 and 0.9 respectively.

### 2.5. Distribution coefficient ( $K_D$ ) studies

$K_D$  values were obtained using the batch contact method. 20 mg of AM resin was prepared in 1.5 mL Eppendorf vials. Stock solutions for each metal were prepared by diluting High Purity ICP standards (100 ppm for Sc and 1000 ppm for Ti, both in 2%  $\text{HNO}_3$ ) in HCl at various concentrations (0.5, 1, 2, 4, 8 and 10.8 M) to a final concentration of 10 ppm. Initial studies were conducted by first drying down the ICP standards and re-dissolving in the appropriate HCl concentration, but the results did not vary statistically from those obtained by the direct dilution method, so it was determined that the small amount of  $\text{HNO}_3$  present in the initial metal solutions did not affect or contribute to the resulting distribution coefficients. 1 mL of these standard solutions was then added to the vials containing the resin which were then sealed and mixed by inversion at room temperature for 24 h to allow for equilibration. Following mixing, the tubes were centrifuged and a 500  $\mu\text{L}$  aliquot obtained, diluted in 2%  $\text{HNO}_3$  and submitted for ICP-OES analysis (Supplementary Materials) to determine the concentration of analyte remaining in the aqueous phase. This was compared to the concentration of the initial cold metal standard and the distribution coefficient calculated using the following equation, where  $C_B$  and  $C_A$  are the elemental concentrations of the analyte in solution before and after equilibrium respectively (Equation (1)). Each experiment was done in triplicate at each concentration range.

$$K_D = \frac{(C_B - C_A)/V}{C_A/V} \quad (1)$$

## 2.6. Preparation and evaluation of generators

10 mL tapered Bio-Rad® columns were rinsed with Chelex purified water and filled to the appropriate bed volume (BV) with the corresponding resin that had been weighed and slurried in Chelex purified water. A small piece of glass wool was added to the top of the resin for protection, and the column washed with Chelex purified water and 2 M HCl. A sample of  $^{44}\text{Ti}$  was evaporated to dryness, reconstituted with 2 M HCl, and loaded onto the columns by volumetric pipette. The solutions were allowed to elute by gravity. The generators were eluted 5 times per week with 4 BV of dilute HCl (2 M or 0.5 M), and an aliquot was counted by HPGe (Supplementary Materials).

## 2.7. Total organic content (TOC) studies

10 mL tapered Bio-Rad® columns were rinsed with Chelex purified water and filled to a bed volume (BV) of 300  $\mu\text{L}$  with the corresponding resin that had been weighed and slurried in Chelex purified water. Two columns were prepared with the ZR resin and two were prepared with the synthesized AM resin. One of each type of resin column was rinsed with 50 BV of 0.5 M HCl and the other two remaining columns with each type of resin was eluted with 50 BV of 2 M HCl. Samples were collected after 10, 20, 30, 40, and 50 BV of eluent and sent for total organic content (TOC) analysis at Long Island Analytical Laboratories Inc. (Holbrook, New York 11741). A blank of each acid used (0.5 and 2 M HCl) was also sent for analysis for comparison.

## 3. Results and discussion

### 3.1. Resin synthesis and characterization

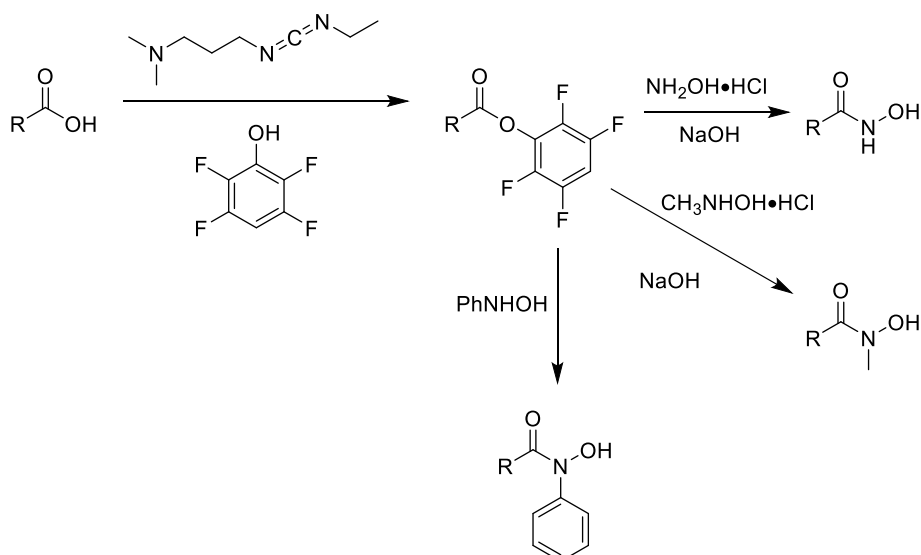
The unsubstituted hydroxamate Accell resin was prepared following modified literature procedures (Holland et al., 2009; Meijs et al., 1994; Phillips and Fritz, 1982) by functionalizing the carboxylate groups of the Accell resin first to an ester, followed by conversion to the hydroxamate by reaction with hydroxylamine hydrochloride. The N-methylhydroxamate resin (AM) can be synthesized using the same procedure substituting hydroxylamine hydrochloride for N-methylhydroxylamine hydrochloride. The N-phenylhydroxamate Accell resin (AP) can be synthesized from the ester functionalized resin using a similar procedure, but without the use of NaOH, as the N-phenylhydroxylamine is already in the free base form (Scheme 1). Addition of 1.0 mL of NaOH to the N-phenylhydroxylamine resin reaction results in hydrolysis of the

ester resin back to the carboxylate form.

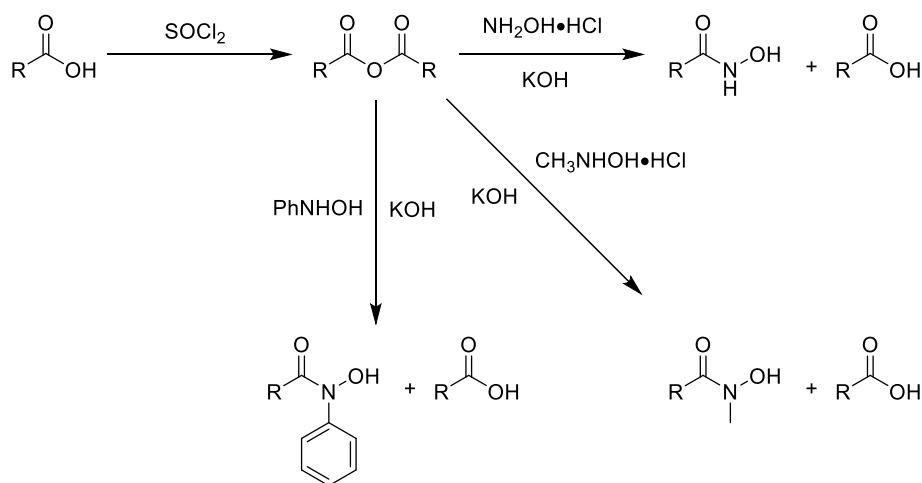
The characterization of the Accell resins by ATIR was difficult due to weak signal intensities caused by low ligand density and the overpowering silica peaks of the resin backbone, resulting in only the carbonyl region of the IR spectra being used in characterization. The starting Accell carboxylate resin shows asymmetric ( $\nu_{\text{as}}$ ) and symmetric ( $\nu_{\text{s}}$ ) C=O stretching frequencies at  $1562\text{ cm}^{-1}$  and  $1408\text{ cm}^{-1}$  respectively. In the intermediate ester resin this C=O stretching frequency shifts to higher energy at  $1781\text{ cm}^{-1}$ . All three hydroxamate resins show a diagnostic C=O stretching frequency signal around  $1730\text{ cm}^{-1}$  as well as a second peak at around  $1450\text{ cm}^{-1}$ , there is also evidence for the  $\nu_{\text{as}}$  and  $\nu_{\text{s}}$  carboxylate C=O peaks at approximately  $1550\text{ cm}^{-1}$  and  $1400\text{ cm}^{-1}$  respectively. There is no evidence of the carboxylate peaks in the ester resin, suggesting that there is some hydrolysis of the ester in the hydroxylamine reaction. The peaks seen at approximately  $3400$ ,  $1650$ ,  $1065$ ,  $960$ ,  $800$  and  $450\text{ cm}^{-1}$  in the Accell resin spectra are assigned as silica peaks, this was confirmed by direct comparison with the IR spectrum of crude silica gel. Formation of the hydroxamate functional group was also verified qualitatively by the visual formation of a dark red complex upon addition of Fe(III) in dilute acid to the resin (Davidson, 1940).

The procedure for the synthesis of the IRC50 and CG50 hydroxamate resins are the same as each other but differ from that of the Accell resin. Attempts to use the same procedure as described above using IRC50 or CG50 resin did not result in formation of the ester functionalized resin in the first step, but rather formation of an anhydride. This was determined by characterization of the intermediate product using IR, which showed two diagnostic C=O stretching frequencies at  $1800\text{ cm}^{-1}$  and  $1750\text{ cm}^{-1}$ , this was true for both the IRC50 and CG50 resins. An alternate route to hydroxamate synthesis is conversion of carboxylates into acid chlorides which are then reacted with hydroxylamine, this has been suggested in the literature for similar resins (Cornaz et al., 1957; Phillips and Fritz, 1980, 1982; Petrie et al., 1965; Liu et al., 1992). Reaction of IRC50 and CG50 with  $\text{SOCl}_2$  under reflux resulted in the same anhydride product that was observed in the ester formation attempt (Scheme 2), this was evident by the identical IR spectrum of the product. Due to the high ligand density of the resins and the close contact of the neighboring carboxylate groups, all attempts at formation of the acid chlorides or esters (as in the Accell resin synthesis) always resulted in formation of the anhydride derivative without any apparent formation of the ester or acid chloride in any appreciable amounts.

There is literature evidence that it is possible to convert anhydrides into a 1:1 mix of hydroxamates and carboxylic acids by reaction with the



Scheme 1. Synthesis of Accell based hydroxamate resins.



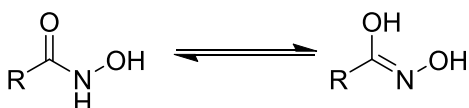
Scheme 2. Synthesis of IRC50 and CG50 based hydroxamate resins.

free-based hydroxylamine and base (Wong et al., 2019; Reddy et al., 2000). Based on this, the hydroxamate IRC50 and CG50 resins were synthesized using modified literature procedures using the anhydride resin (Scheme 2). (Renfrow and Hauser, 1937; Liu et al., 1992; Wong et al., 2019) The hydroxylamine hydrochloride and N-methylhydroxylamine hydrochloride were free-based by reaction with one equivalent of KOH in MeOH, followed by removal of the KCl salt. This MeOH hydroxylamine solution was then added to the dry anhydride resin and allowed to react for 1 h at room temperature. An additional molar equivalent of KOH in MeOH was then added briefly to catalyze the reaction to completion, but it was found that prolonged exposure of the hydroxamate resin to base resulted in hydrolysis back to the starting carboxylate resin. This product is presumably the potassium salt of the resin, so to protonate the hydroxamate groups the resin was washed in 0.1 M HCl. Exposure of this resin to  $\geq 1$  M HCl solutions resulted in hydrolysis of the hydroxamates back to carboxylates. While the N-phenylhydroxylamine is already in the free base form and can be directly dissolved and reacted with the anhydride resin, catalytic amount of KOH is necessary after the initial 1-h reaction to aid in product formation.

All six of these resins form dark red complexes in dilute acid solution with Fe(III) suggesting successful formation of the hydroxamate group. The IR spectra of resins show peaks due to both the carboxylate groups as well as the hydroxamate groups, with the C=O stretching frequency of the hydroxamate found around  $1720\text{ cm}^{-1}$  in all six resins. With the unsubstituted hydroxamate IRC50 and CG50 resins there was also occasionally a peak around  $1680\text{ cm}^{-1}$  (and no peak at  $1720\text{ cm}^{-1}$ ) that was not seen in the N-methyl or N-phenyl derivatives. This is likely due to the C=N stretching frequency that is present in the equilibria structure of the unsubstituted hydroxamate (Scheme 3).. (Higgins et al., 2006)

### 3.2. $K_D$ studies of AM resin

Results of the distribution coefficient studies of Sc and Ti on the AM resin in varying concentration of HCl is shown in Fig. 1. As can be seen clearly in the plot, Ti is strongly retained on the resin across all HCl concentrations with  $K_D$  values above 7000 across acid concentrations from 0.5 to 8 M, and a slight decrease to 5000 for the higher



Scheme 3. Equilibria structures of an unsubstituted hydroxamate functional group.

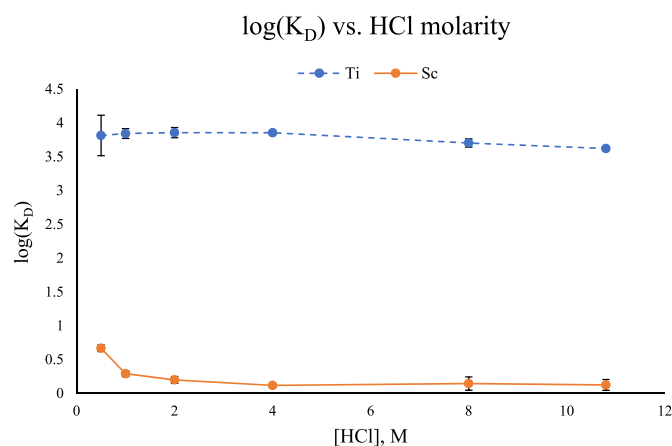


Fig. 1. Ti and Sc distribution coefficient dependencies on HCl concentration for AM resin.

concentrations (8 and 10.8 M). Sc alternatively shows little to no retention across all HCl concentrations, all  $K_D$  values for Sc are below 2, except for 0.5 M HCl which is slightly increased to a  $K_D$  value around 4. These values are an improvement for both retention of Ti and weak affinity of Sc compared to the hydroxamate based ZR resin across a similar range of HCl concentrations (Radchenko et al., 2016). The slight increase of  $K_D$  values for Sc at low acid concentrations (0.5 M HCl) suggests that further dilute solutions of HCl ( $< 0.5$  M) may not be suitable to obtain appreciable amount of Sc from the resin in small volumes, but the large separation factor between Ti and Sc across all HCl concentrations tested here is extremely promising that this resin will be a good candidate for a  $^{44}\text{Ti}/^{44}\text{Sc}$  radionuclide generator.

### 3.3. Generator performance

Small-scale generators comprised of all nine of the synthesized hydroxamate resins were prepared in columns using a 300  $\mu\text{L}$  BV and were loaded on the same day with 740 kBq (20  $\mu\text{Ci}$ ) of  $^{44}\text{Ti}$ , as well as three 300  $\mu\text{L}$  BV “blank” generators loaded with 481 kBq (13  $\mu\text{Ci}$ ) of  $^{44}\text{Ti}$  using the same procedure with unmodified IRC50, CG50 and Accell resins. These blanks were tested to ensure that the carboxylate groups of the starting resin were not contributing to any metal binding seen in the hydroxamate resins. All nine synthesized resins were tested in addition to the commercially available ZR resin, the mass of resin used in each generator is given in Table 1. All generators were subsequently eluted with four bed volumes of 0.5 M HCl daily (or 5 times per week for the

**Table 1**  
Mass of resins used for 300  $\mu$ L BV generator in a 10 mL tapered column.

Resin	Mass (mg)			
	Blank	Unsubstituted	Methyl	Phenyl
Accell	115	125	120	110
IRC50	110	170	160	150
CG50	80	100	105	110
ZR		80		

longer lasting generators) to monitor the amount of  $^{44}\text{Sc}$  eluted as well as any  $^{44}\text{Ti}$  breakthrough.

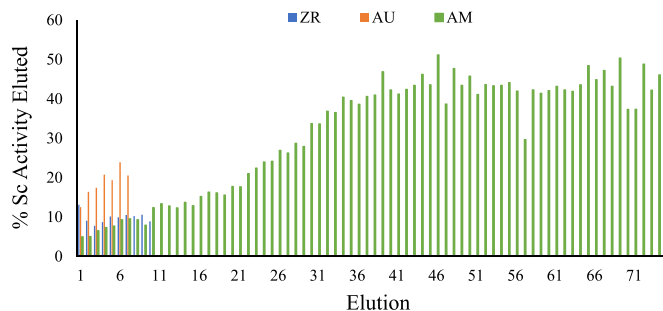
Unsurprisingly all unfunctionalized “blank” resins (in the carboxylate form) showed complete  $^{44}\text{Ti}$  breakthrough during the load and failed to bind appreciable amounts of Ti. For the remaining resins, it was found that all functionalized IRC50 and CG50 resins failed to bind the Ti and displayed complete  $^{44}\text{Ti}$  breakthrough either during the load or in the subsequent elution (Elute 1) (Table 2). This is likely due to hydrolysis of the hydroxamate groups in the 2 M HCl as described previously. Similar results were found by Holland et al. with the unsubstituted Accell based hydroxamate resin, where the loading  $^{89}\text{Zr}(\text{IV})$  efficiency was found to be  $>99.9\%$  at HCl concentrations of  $\leq 2$  M, but at higher concentrations the binding affinity of the resin decreases drastically (Holland et al., 2009). The AU and AM resins, however, displayed 100%  $^{44}\text{Ti}$  loading efficiency, and the ZR resin showed a small amount of  $^{44}\text{Ti}$  breakthrough during the load leading to 93.5%  $^{44}\text{Ti}$  loading efficiency (Table 2).

The ZR, AU and AM generators were eluted daily with 4 bed volumes of 0.5 M HCl. The resulting  $^{44}\text{Sc}$  activity eluted as well as any potential  $^{44}\text{Ti}$  breakthrough was monitored through HPGe  $\gamma$  spectroscopy. The AU generator displayed the highest eluted  $^{44}\text{Sc}$  activity, almost double that of the ZR and AM generators, but was also the first to display  $^{44}\text{Ti}$  breakthrough. The AU generator was eluted seven times (total 28 BV) over seven days before 0.45%  $^{44}\text{Ti}$  breakthrough was observed on the 8th day and was no longer eluted. The ZR generator was eluted 10 times (total 40 BV) over 10 days before 0.16%  $^{44}\text{Ti}$  breakthrough was observed. The AM generator was eluted 75 times (total 300 BV) over several months before breakthrough was observed. The lifetime of the generator using the Accell methyl hydroxamate resin is almost seven times longer than the ZR resin generator, and overall showed increased  $^{44}\text{Sc}$  activity elution under the same conditions. The elution profile of these three generators is displayed in Graph 1. Over the elution period of the AM generator there was a steady increase of  $^{44}\text{Sc}$  activity eluted from 10% to a maximum of 50%. After this slow increase the elution activity seemed to plateau and remain constant around 40–50%. The reason behind this increasing eluted activity trend is still unknown, although it is hypothesized to be due to protonation of open hydroxamate sites over time by the eluting acid allowing for more  $^{44}\text{Sc}$  to be eluted and not

**Table 2**  
2 M HCl generator experiment evaluating  $^{44}\text{Ti}$  breakthrough in load and first elution.

Resin	% Ti Breakthrough	
	Load	Elute 1
Accell Blank	100	–
IRC50 Blank	97	–
CG50 Blank	100	–
ZR	6.5	0
AU	0	0
AM	0	0
AP	72	18
IU	96	3
IM	100	–
IP	72	26
CU	93	4
CM	100	–
CP	100	–

## Generator Elution Profile Comparison



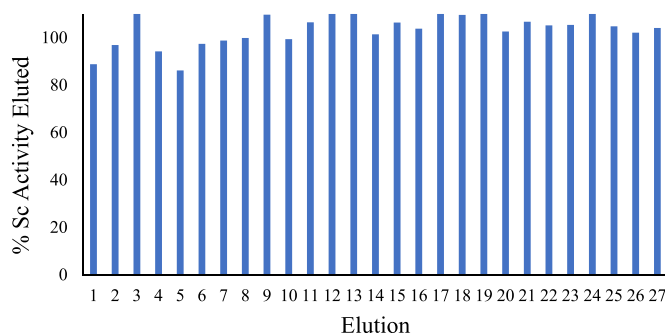
**Graph 1.** Elution profile of small-scale generators.

captured by open sites. If the reason for the increasing  $^{44}\text{Sc}$  activity was due to the movement of  $^{44}\text{Ti}$  down the column thereby movement of the  $^{44}\text{Sc}$  towards the end of the column then we would expect to observe  $^{44}\text{Ti}$  breakthrough shortly after the maximum  $^{44}\text{Sc}$  activity was reached, which was not observed. Further studies are needed to ascertain the cause of this observed elution trend.

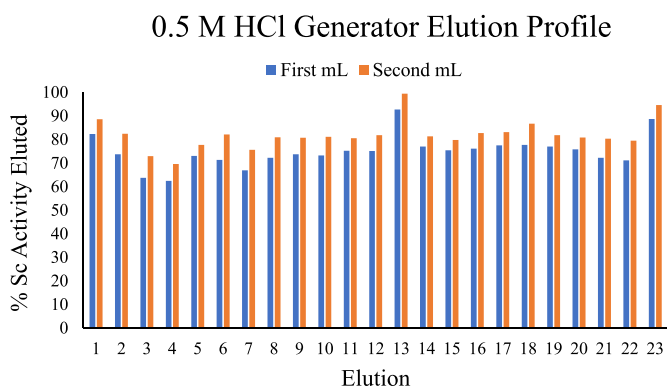
A scaled-up generator experiment was similarly conducted using the AM resin to test the system in a more clinically relevant scale as it showed extremely promising results in the small scale 740 kBq (20  $\mu$ Ci) generator study. A 1 mL BV column (0.400 g AM resin) was loaded with 37 MBq (1 mCi) of  $^{44}\text{Ti}$  in 2 M HCl. The generator was eluted daily with 4 BV of 2 M HCl and the fractions counted to monitor the  $^{44}\text{Sc}$  elution activity as well as any potential  $^{44}\text{Ti}$  breakthrough. The elution profile of this generator is shown below in Graph 2. Remarkably, this generator showed consistent quantitative elution of  $^{44}\text{Sc}$  on a daily basis using the same volume of eluent (normalized to the column BV) as the small-scale study. The drastic increase in eluted activity may be due to the increased activity:resin ratio, by loading a larger amount of  $^{44}\text{Ti}$  onto a smaller mass of resin there may be less coordination sites open to bind the free  $^{44}\text{Sc}$  making it more facile to elute. The lack of  $^{44}\text{Ti}$  breakthrough observed in the loading procedure suggests that the loading capacity of the resin was not saturated, so it may be possible to load even higher activities onto a 1 mL BV of AM resin. Further studies are needed to determine the saturation point of the resin and what affect this has on subsequent  $^{44}\text{Sc}$  elution behavior.

Attempts to further improve this generator towards direct radiolabeling conditions were conducted by eluting in more dilute HCl. A 0.5 mL BV column (0.200 g AM resin) was loaded in 2 M HCl with 37 MBq (1 mCi) of  $^{44}\text{Ti}$  and then eluted daily with 4 BV of 0.5 M HCl. The elution profile of this generator is shown in Graph 3. This generator consistently eluted 80–85%  $^{44}\text{Sc}$  in the 4 BV fractions (2 mL), with 90% of this activity being eluted in the first 1 mL allowing for isolation of 28–30 MBq (750–800  $\mu$ Ci) of  $^{44}\text{Sc}$  in 1 mL of 0.5 M HCl. Thus, producing a scandium product which should be highly favorable for use in direct radiolabeling

## 2 M HCl Generator Elution Profile



**Graph 2.** Elution profile of 2 M HCl 37 MBq AM generator.



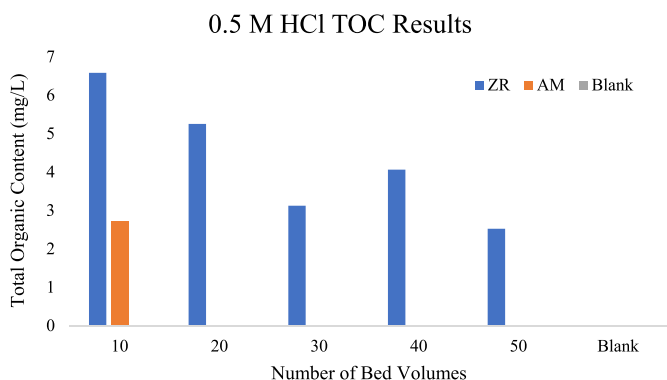
**Graph 3.** Elution profile of 0.5 M HCl 37 MBq AM generator shown as activity obtained in the first 1 mL fraction and the second 1 mL fraction.

experiments.

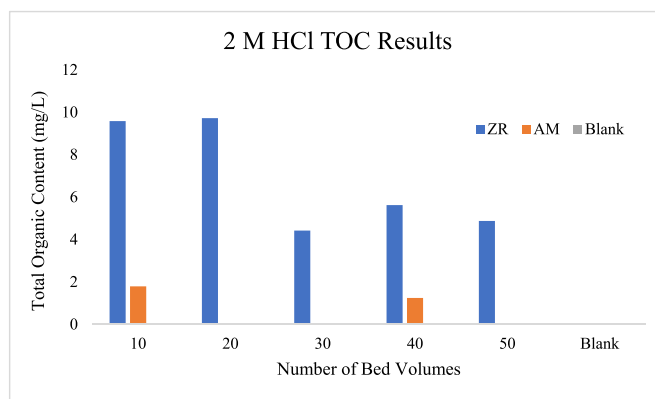
From the generator studies that have been conducted to date using the AM resin, there has not been any observation of resin degradation or structural damage from radiation from the <sup>44</sup>Ti or <sup>44</sup>Sc, even in the higher activity 1 mCi generators. There is a risk that with higher activity generators the hydroxamate-based resin may undergo radiolytic damage from the high energy gammas from <sup>44</sup>Sc or the positron emission, but further studies are needed. Future work will include preparation of higher, more clinically relevant activity generators to determine viability and potential degradation to the resin from the intense radiation environment.

### 3.4. Total organic content

To determine and compare the amount of organic impurities that are potentially being eluted from the extraction chromatographic ZR resin and the covalently bound synthesized AM resin, small columns containing the resin were prepared and eluted with 0.5 M and 2 M HCl. The eluent was collected and sent for total organic content analysis. The results of the analysis are shown below, the 0.5 M HCl in Graph 4 and the 2 M HCl in Graph 5. In both cases the acid used did not show any organic content in the blank samples and therefore did not contribute to any organic content found in the column eluent samples. For both acid concentrations there is considerably more organic impurities being eluted from the ZR resin column, where there is little to no organic impurities being eluted from the AM resin columns. These results suggest that <sup>44</sup>Sc eluted from an AM resin generator has the potential to be directly radiolabeled without any post-elution processing or purification as there are no organic impurities being eluted from the resin itself that would inhibit <sup>44</sup>Sc radiolabeling.



**Graph 4.** Total organic content analysis of 0.5 M HCl eluent from ZR and AM resin columns.



**Graph 5.** Total organic content analysis of 2 M HCl eluent from ZR and AM resin columns.

### 3.5. Specific activity of generator produced <sup>44</sup>Sc

To determine the specific activity of the AM resin generator produced <sup>44</sup>Sc, the eluted fractions from the 1 mCi 2 M HCl eluted generator were collected and analyzed by ICP-OES (Supplementary Materials) to determine the amount of cold Sc in the collected eluent. All four fractions from each elution 1, 5, 10, 15, 20 and 25 were combined, diluted to 8 mL in 2% HNO<sub>3</sub> and each analyzed by ICP-OES. The analyzed Sc peaks from elution 20 had an RSD of 43% so no reliable data was obtained, but all remaining elution samples had RSD values below 10% and the resulting Sc concentration and amount are given in Table 3.

These results demonstrate that there is very little cold scandium in the eluted fractions from the AM resin generator, suggesting that the eluted <sup>44</sup>Sc is carrier free, or at the very least that the amount of cold scandium in the elutions is below the detection limit of the ICP-OES.

### 3.6. Radiolabeling

One of the biggest drawbacks to currently employed <sup>44</sup>Sc generators is that the eluent needs post-elution purification in order to use the <sup>44</sup>Sc in subsequent radiolabeling reactions (Pruszyński et al., 2010). This is due to the presence of competing chelators in the eluent such as the oxalates present in oxalic acid. To overcome this, current methods employ the use of a second column to purify the <sup>44</sup>Sc by removal of the oxalates and isolation of the <sup>44</sup>Sc in a radiolabeling conducive buffer. To avoid post-elution processing of the generator eluent and allow for direct radiolabeling of the <sup>44</sup>Sc several criteria need to be met: the eluent must be free of competing chelators, the eluent must not be highly acidic, and

**Table 3**  
Resulting scandium ICP-OES data from 1 mCi 2 M HCl generator elutions.

	Combined fractions volume (mL)	ICP sample Sc concentration (ppm)	Combined fractions Sc concentration (ppm)	Amount of Sc in combined fractions (mg)	% RSD
Elution 1	3.885	0.001	0.0021	0.008	1.03
Elution 5	3.195	0.001	0.0025	0.008	1.09
Elution 10	3.374	0	0 <sup>a</sup>	0 <sup>a</sup>	9.14
Elution 15	4.148	0	0 <sup>a</sup>	0 <sup>a</sup>	8.11
Elution 20	3.129	0	–	–	43.41
Elution 25	3.633	0.001	0.0022	0.008	2.45

<sup>a</sup> Below detection limit of machine.

the volume:activity ratio must be low in order to keep radiolabeling reaction total volumes reasonable. The generator presented in this work meets all of these criteria and should allow for use of the eluted  $^{44}\text{Sc}$  directly from the generator without the need of time-consuming post-elution processing and loss of activity.

To test this, preliminary radiolabeling studies were conducted on the generator eluent from the 37 MBq (1 mCi) generator eluted with 0.5 M HCl with DOTA under standard radiolabeling conditions. The  $^{44}\text{Sc}$  was obtained in 0.5 M HCl and then brought to a pH of 4 with the addition of 0.5 M NaOH. This solution was then added directly to an Eppendorf vial containing DOTA stock solution in 0.25 M  $\text{NH}_4\text{OAc}$  at a pH of 4, with a resulting pH of 4 for the reaction solution. The solution was heated at 90 °C for 60 min and the radioyield determined by iTLC. This reaction was conducted using 925 kBq (25  $\mu\text{Ci}$ ) of  $^{44}\text{Sc}$  and 1.59 nmol of DOTA resulting in a  $99.24 \pm 0.21\%$  yield, which is consistent with other generator produced  $^{44}\text{Sc}$  samples that have been processed using chromatography post-elution (Kerdjoudj et al., 2016). More studies are needed to further optimize and study the radiolabeling efficiencies of this generator produced  $^{44}\text{Sc}$ , but these preliminary results show extremely promising evidence for the ability to directly radiolabel  $^{44}\text{Sc}$  from this generator system.

#### 4. Conclusion

Several hydroxamate-based resins were synthesized and tested for use in  $^{44}\text{Ti}/^{44}\text{Sc}$  generator systems. The methylated Accell-based hydroxamate resin proved the most successful in terms of lifetime before  $^{44}\text{Ti}$  breakthrough and showed enhanced properties over the commercially available alternative ZR resin. The ability to elute the generator with small volumes of 0.5 M HCl also enabled the use of the generator produced  $^{44}\text{Sc}$  in direct radiolabeling reactions with DOTA under standard conditions, which is not possible with current anion exchange resin generators in the literature (Filosofov et al., 2010; Larenkov et al., 2021). While these results are preliminary and further studies and optimizations of this generator system are needed, these results show extremely promising data that this new resin may be especially useful as a resin matrix for a more clinically viable  $^{44}\text{Ti}/^{44}\text{Sc}$  generator system.

#### CRedit authorship contribution statement

**Leah Gajecski:** Writing – original draft, Validation, Methodology, Investigation, Conceptualization. **Celine M. Marino:** Writing – review & editing, Investigation. **Cathy S. Cutler:** Writing – review & editing. **Vanessa A. Sanders:** Writing – review & editing, Supervision, Project administration, Funding acquisition.

#### Declaration of competing interest

The authors declare that they have no known competing financial interests or personal relationships that could have appeared to influence the work reported in this paper.

#### Data availability

Data will be made available on request.

#### Acknowledgments

The authors would like to thank the Department of Energy Core R&D Funding (ST5001030) for their generous support.

#### Appendix A. Supplementary data

Supplementary data to this article can be found online at <https://doi.org/10.1016/j.apradiso.2022.110588>.

#### References

- Agrawal, Y.K., Kaur, H., Menon, S.K., 1999. Poly(styrene-p-hydroxamic acids): synthesis, and ion exchange separation of rare earths. *React. Funct. Polym.* 39, 155–164.
- Brennan, B.J., Chen, J., Rudshsteyn, B., Chaudhuri, S., Mercado, B.Q., Batista, V.S., Crabtree, R.H., Brudvig, G.W., 2016. Molecular titanium-hydroxamate complexes as models for  $\text{TiO}_2$  surface binding. *Chem. Commun.* 52, 2972–2975.
- Cornaz, J.-P., Hutschneker, K., Deuel, H., 1957. Säurechloride und Hydroxamsäuren von Carboxyl-Ionenaustauschern. 10. Mitteilung über Ionenaustauscher. *Helv. Chim. Acta* 40, 2015–2019.
- Cornaz, J.P., Deuel, H., 1954. Selektive Ionenaustauscher für  $\text{Fe}^{3+}$ . *Experientia* 10, 137–138.
- Davidson, D., 1940. Hydroxamic acids in qualitative organic analysis. *J. Chem. Educ.* 17, 81.
- Dirks, C.B.A., Maudoux, N., 2015. On the Development and Characterisation of an Hydroxamate Based Extraction Chromatographic Resin. *61st Radiobiology and Radiochemistry Measurements Conference*. Iowa City, IA, USA.
- Domnanich, K.A., Muller, C., Farkas, R., Schmid, R.M., Ponsard, B., Schibli, R., Turler, A., VAN DER Meulen, N.P., 2017.  $^{44}\text{Sc}$  for labeling of DOTA- and NODAGA-functionalized peptides: preclinical in vitro and in vivo investigations. *EJNMMI Radiopharm Chem* 1, 8.
- Eigner, S., Vera, D.R.B., Fellner, M., Loktionova, N.S., Piel, M., Lebeda, O., Rösch, F., Roß, T.L., Henke, K.E., 2013. Imaging of protein synthesis: in vitro and in vivo evaluation of  $^{44}\text{Sc}$ -DOTA-Puromycin. *Mol. Imag. Biol.* 15, 79–86.
- Filosofov, D.V., Loktionova, N.S., Rösch, F., 2010. A  $^{44}\text{Ti}/^{44}\text{Sc}$  radionuclide generator for potential application of  $^{44}\text{Sc}$ -based PET-radiopharmaceuticals. *ra - Radiochimica Acta* 98, 149–156.
- Hernandez, R., Valdovinos, H.F., Yang, Y., Chakravarty, R., Hong, H., Barnhart, T.E., Cai, W., 2014.  $^{44}\text{Sc}$ : an attractive isotope for peptide-based PET imaging. *Mol. Pharm.* 11, 2954–2961.
- Herscheid, J.D., Vos, C.M., Hoekstra, A., 1983. Manganese-52m for direct application: a new  $^{52}\text{Fe}/^{52}\text{mMn}$  generator based on a hydroxamate resin. *Int. J. Appl. Radiat. Isot.* 34, 883–886.
- Higgins, F.S., Magliocco, L.G., Colthup, N.B., 2006. Infrared and Raman spectroscopy study of alkyl hydroxamic acid and alkyl hydroxamate isomers. *Appl. Spectrosc.* 60, 279–287.
- Holland, J.P., Sheh, Y., Lewis, J.S., 2009. Standardized methods for the production of high specific-activity zirconium-89. *Nucl. Med. Biol.* 36, 729–739.
- Honarvar, H., Müller, C., Cohrs, S., Haller, S., Westerlund, K., Karlström, A.E., VAN DER Meulen, N.P., Schibli, R., Tolmachev, V., 2017. Evaluation of the first  $^{44}\text{Sc}$ -labeled Affibody molecule for imaging of HER2-expressing tumors. *Nucl. Med. Biol.* 45, 15–21.
- Jones, K.E., Batchler, K.L., Zalouk, C., Valentine, A.M., 2017.  $\text{Ti(IV)}$  and the siderophore desferrioxamine B: a tight complex has biological and environmental implications. *Inorg. Chem.* 56, 1264–1272.
- Kerdjoudj, R., Pniok, M., Alliot, C., Kubíček, V., Havlíčková, J., Rösch, F., Hermann, P., Huclier-Markai, S., 2016. Scandium(III) complexes of monophosphorus acid DOTA analogues: a thermodynamic and radiolabelling study with  $^{44}\text{Sc}$  from cyclotron and from a  $^{44}\text{Ti}/^{44}\text{Sc}$  generator. *Dalton Trans.* 45, 1398–1409.
- Khodadadi, R., Fakhri, S., Entezami, A.A., 1995. Poly(hydroxamic Acid) Chelating Resin: The Synthesis and Uses.
- Koumariou, E., Loktionova, N.S., Fellner, M., Roesch, F., Thews, O., Pawlak, D., Archimandritis, S.C., Mikolajczak, R., 2012.  $^{44}\text{Sc}$ -DOTA-BN[2-14]NH<sub>2</sub> in comparison to  $^{68}\text{Ga}$ -DOTA-BN[2-14]NH<sub>2</sub> in pre-clinical investigation. Is  $^{44}\text{Sc}$  a potential radionuclide for PET? *Appl. Radiat. Isot.* 70, 2669–2676.
- Larenkov, A.A., Makichyan, A.G., Iatsenko, V.N., 2021. Separation of  $^{44}\text{Sc}$  from  $^{44}\text{Ti}$  in the context of A generator system for radiopharmaceutical purposes with the example of  $^{44}\text{Sc}$ -PSMA-617 and  $^{44}\text{Sc}$ -PSMA-1& T synthesis. *Molecules* 26, 6371.
- Liu, C.Y., Chen, M.J., Lee, N.M., Hwang, H.C., Jou, S.T., Hsu, J.C., 1992. Synthesis and coordination behavior of hydroxamate resin with varying spacer groups. *Polyhedron* 11, 551–558.
- Mawji, E., Gledhill, M., Milton, J.A., Tarran, G.A., Usher, S., Thompson, A., Wolff, G.A., Worsfold, P.J., Achterberg, E.P., 2008. Hydroxamate siderophores: occurrence and importance in the Atlantic ocean. *Environ. Sci. Technol.* 42, 8675–8680.
- Meijs, W.E., Herscheid, J.D.M., Haisma, H.J., Wijbrandts, R., VAN Langevelde, F., VAN Leuffen, P.J., Mooy, R., Pinedo, H.M., 1994. Production of highly pure no-carrier added  $^{89}\text{Zr}$  for the labelling of antibodies with a positron emitter. *Appl. Radiat. Isot.* 45, 1143–1147.
- Orlowska, E., Roller, A., Wiesinger, H., Pignitter, M., Jirsa, F., Krachler, R., Kandioller, W., Keppler, B.K., 2016. Benzoic hydroxamate-based iron complexes as model compounds for humic substances: synthesis, characterization and algal growth experiments. *RSC Adv.* 6, 40238–40249.
- Padial, N.M., Castells-Gil, J., Almora-Barrios, N., Romero-Angel, M., Da Silva, I., Barawi, M., García-Sánchez, A., DE LA Peña O'Shea, V.A., Martí-Gastaldo, C., 2019. Hydroxamate titanium-organic frameworks and the effect of siderophore-type linkers over their photocatalytic activity. *J. Am. Chem. Soc.* 141, 13124–13133.
- Passadis, S.S., Hadjithoma, S., Sifarika, P., Kalampounias, A.G., Keramidas, A.D., Miras, H.N., Kabanos, T.A., 2021. Synthesis, structural and physicochemical characterization of a titanium(IV) compound with the hydroxamate ligand N,2-Dihydroxybenzamide. *Molecules* 26, 5588.

- Petrie, G., Locke, D., Meloan, C.E., 1965. Hydroxamic acid chelate ion exchange resin. *Anal. Chem.* 37, 919–&.
- Phillips, R.J., 1980. Chelating ion exchange with macroreticular hydroxamic acid resins. Doctor of Philosophy, Iowa State University.
- Phillips, R.J., Fritz, J.S., 1980. Synthesis and analytical properties of an n-phenyl-hydroxamic acid resin. *Anal. Chim. Acta* 121, 225–232.
- Phillips, R.J., Fritz, J.S., 1982. Extraction of metal ions by N-phenyl-, N-methyl-, and N-unsubstituted hydroxamic acid resins. *Anal. Chim. Acta* 139, 237–246.
- Pruszyński, M., Loktionova, N.S., Filosofov, D.V., Rösch, F., 2010. Post-elution processing of  $^{44}\text{Ti}/^{44}\text{Sc}$  generator-derived  $^{44}\text{Sc}$  for clinical application. *Appl. Radiat. Isot.* 68, 1636–1641.
- Radchenko, V., Meyer, C.A.L., Engle, J.W., Naranjo, C.M., Unc, G.A., Mastren, T., Brugh, M., Birnbaum, E.R., John, K.D., Nortier, F.M., Fassbender, M.E., 2016. Separation of  $^{44}\text{Ti}$  from proton irradiated scandium by using solid-phase extraction chromatography and design of  $^{44}\text{Ti}/^{44}\text{Sc}$  generator system. *J. Chromatogr. A* 1477, 39–46.
- Reddy, A.S., Kumar, M.S., Reddy, G.R., 2000. A convenient method for the preparation of hydroxamic acids. *Tetrahedron Lett.* 41, 6285–6288.
- Renfrow, W.B., Hauser, C.R., 1937. The relative rates of decomposition of the potassium salts of certain meta and para substituted dibenzhydroxamic acids. A study of the lossen Rearrangement<sup>1,2</sup>. *J. Am. Chem. Soc.* 59, 2308–2314.
- Roesch, F., 2012. Scandium-44: benefits of a long-lived PET radionuclide available from the  $(^{44}\text{Ti})/(^{44}\text{Sc})$  generator system. *Curr. Rad.* 5, 187–201.
- Saxena, M., Loza-Rosas, S.A., Gaur, K., Sharma, S., Pérez Otero, S.C., Tinoco, A.D., 2018. Exploring titanium(IV) chemical proximity to iron(III) to elucidate a function for Ti (IV) in the human body. *Coord. Chem. Rev.* 363, 109–125.
- Szanişzlo, P.J., Powell, P.E., Reid, C.P.P., Cline, G.R., 1981. Production of hydroxamate siderophore iron chelators by ectomycorrhizal Fungi. *Mycologia* 73, 1158–1174.
- Wong, P.T., Bhattacharjee, S., Cannon, J., Tang, S., Yang, K., Bowden, S., Varnau, V., O'Konek, J.J., Choi, S.K., 2019. Reactivity and mechanism of  $\alpha$ -nucleophile scaffolds as catalytic organophosphate scavengers. *Org. Biomol. Chem.* 17, 3951–3963.